JOURNAL OF Materials CHEMISTRY

Real-time holographic grating by means of photoresponsive polymer liquid crystals with a flexible siloxane spacer in the side chain

Makoto Hasegawa,[a] Takahiro Yamamoto,[a] Akihiko Kanazawa,[a] Takeshi Shiono,[a] Tomiki Ikeda,[a] Yu Nagase,[b] Eiichi Akiyama[b] and Yuriko Takamura[b]

[a]*Research Laboratory of Resources Utilization, Tokyo Institute of Technology, 4259 Nagatsuta, Midori-ku, Yokohama, 226-8503, Japan. E-mail: tikeda@res.titech.ac.jp*
[b]*Sagami Chemical Research Center, 4-4-1 Nishi-Ohnuma, Sagamihara, Kanagawa, 229-0012, Japan*

Received 18th May 1999, Accepted 3rd September 1999

The formation of real-time holographic gratings was investigated in an azobenzene polymer liquid crystal (PLC) possessing a siloxane spacer in the side chain. Irradiation of thin films of the PLCs created a phase grating which is ascribed to periodic induction of the nematic-to-isotropic (N–I) phase transition due to photochemical *trans–cis* isomerization of the azobenzene moiety (photochemical phase transition). It was found that the N–I phase transition temperature of the PLC with the siloxane spacer was lower than that of the PLC without the siloxane spacer owing to flexibility of the siloxane units. This property resulted in a decrease in the irradiation temperature, leading to effective induction of the photochemical N–I phase transition by suppression of thermal *cis–trans* back-isomerization of the azobenzene moiety. Thus formation of the grating in the PLC having the siloxane spacer could be achieved by low intensity of the interference light compared to that in conventional PLCs including only alkyl spacers. Moreover, a grating with narrower fringe spacing could be created by depression of propagation of perturbation due to *trans–cis* photoisomerization of the azobenzene moiety in the LC phase.

Introduction

Much attention has been paid to materials for real-time holography, in which writing and reading of optical information could be performed at the same time, because of its potential for optical communication and information processing. In general, holography records spatial interference patterns generated by the interference of two coherent beams. The interference pattern induces a periodic change in refractive index in the media, resulting in the formation of a so called phase grating hologram. Therefore the property required for real-time holographic materials is a large change in the refractive index by light. For such a material, photoresponsive liquid crystals (LCs) are some of the most promising materials due to their large birefringence based on anisotropic molecular alignment. A particularly exciting advance with respect to holographic materials was reported by Wendorff *et al.* who demonstrated the erasable hologram in polymer liquid crystals (PLCs) containing photochromic molecules.[1–4] Subsequently, many studies relating to the real-time hologram by means of low-molecular-weight liquid crystals (LMWLCs)[5–16] and PLCs[17–19] have been reported by numerous researchers.

We have so far performed systematic studies on the nematic-to-isotropic (N–I) phase transition of polymer liquid crystals (PLCs) containing photochromic molecules such as azobenzene derivatives.[20–29] These chromophores can change their molecular shape upon photoirradiation, which leads to the isothermal N–I phase transition (photochemical phase transition). For example, the *trans* forms of azobenzene derivatives can stabilize the N phase due to their rod-like shape, while the *cis* forms destabilize the N phase because their shape is bent. Therefore, the *trans–cis* photoisomerization of the azobenzene in the N phase can induce disorganization of the LC phase structure. Furthermore, the N phase can be recovered by the thermal *cis–trans* back-isomerization. Recently, the effect of the structure of the side-chain spacer on the photochemical phase transition behavior was explored in the PLCs.[30,31] It was found that introduction of siloxane units as the spacer stabilized the phase structure of the LC phase and depressed the propagation of the perturbation due to *trans–cis* isomerization of the azobenzenes in the LC phase. For the real-time holographic grating, these materials have several advantages in comparison with the conventional PLCs with only alkyl spacers. It is well known that the siloxane spacer results in a decrease in the glass transition temperature and the phase transition temperature of PLCs owing to its flexibility.[32–37] Such properties will lower the irradiation temperature, leading to the suppression of the *cis–trans* thermal back-isomerization. Then the formation of the grating in PLCs with the siloxane spacer will be achieved by light with weak intensity compared to that in the conventional PLCs. Furthermore, formation of a grating with a narrow fringe spacing, *i.e.*, high resolution, can be expected because of suppressed propagation of the perturbation due to the *cis*-azobenzenes. In this paper, formation of the real-time holographic grating by means of PLCs with siloxane spacers in the side chains was investigated, and the effect of the fringe spacing and the beam intensity on the diffraction efficiency was evaluated.

Experimental

Materials

Fig. 1 shows the structure of the PLCs with a siloxane spacer in the side chain (polymer 1) and the corresponding reference analogue without the siloxane spacer (polymer 2) used in the present study. The monomers were prepared according to the synthetic method reported previously.[30,38,39] Each pair of monomers, in which the feed ratio of azobenzene monomers was 25 mol%, and 2,2′-azobisisobutyronitrile (AIBN) were dissolved in dry *N*,*N*-dimethylformamide (DMF) in a polymerization tube. The concentrations of the monomers and AIBN were 500 mmol L^{-1} in total and 25 mmol L^{-1}, respectively. After degassing the mixture, the tube was sealed and

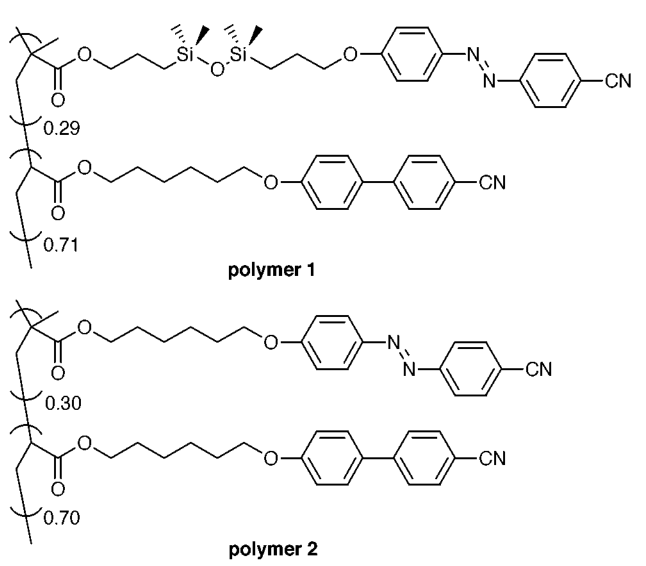

Fig. 1 Structure of polymer liquid crystals used in this study and their abbreviations.

heated at 60 °C for 24 h with stirring. The reaction mixture was then poured into excess methanol to precipitate the polymer. The obtained copolymers, polymer 1 and polymer 2, were reprecipitated twice from their toluene solution into excess methanol and dried *in vacuo* for 24 h. The yields of the polymerizations were 50–60%.

Characterization of PLCs

The composition of the copolymers was determined from a peak intensity in the ^{1}H-NMR spectrum of each monomer unit. ^{1}H-NMR spectra were recorded on a Bruker AM-400 FT-NMR (400 MHz) spectrometer using $CDCl_3$ as the solvent. The number- and weight-average molecular weights (M_n and M_w) of the PLCs were determined by gel permeation chromatography (GPC; Tosoh HLC-802A; column, TSK gel $G5000H_6 + G4000H_6 + G3000H_6 + G2000H_6$; eluent, tetrahydrofuran) calibrated with standard polystyrenes. The phase transition temperature was measured by differential scanning calorimetry (DSC; Seiko Electronic DSC-20 and SSC-580 thermal controller; heating rate, 10 °C min^{-1}), and the phase structure was determined by means of optical polarizing microscopy (Nikon Microphot-UFX; Mettler FP-82 hot stage and Mettler FP-80 central processor) and X-ray diffractometry (MAC Science MXP^3).

Film preparation. Polymer 1 and polymer 2 were dissolved in THF at a low concentration ($\sim 10^{-3}$ mol L^{-1}) and a small portion of the resultant solution was cast on a glass substrate which had been coated with polyimide and rubbed to align mesogens. After the solvent was removed completely under reduced pressure at room temperature, the PLC films were annealed for 12 h at a temperature just below the N-to-I phase transition temperature to yield a monodomain of a well-aligned N phase. The thickness of the LC films was estimated as $\sim$200 nm by absorption spectroscopy on the basis of molar extinction coefficients of the azobenzene moiety.

Measurement

Evaluation of photochemical phase transition behavior. Fig. 2(a) shows the experimental setup used for evaluation of photochemical phase transition behavior of the PLCs under steady-state irradiation. The PLC films were placed in a thermostatted aluminum block and irradiated with an unpolarized Ar$^+$ laser at 488 nm (light intensity, 12 mW cm^{-2}). A He–Ne laser (633 nm) was used as a probe light source and change in the light intensity transmitted through a pair of crossed polarizers, with the sample between them, was measured with a photodiode, and the data were collected with a microcomputer.

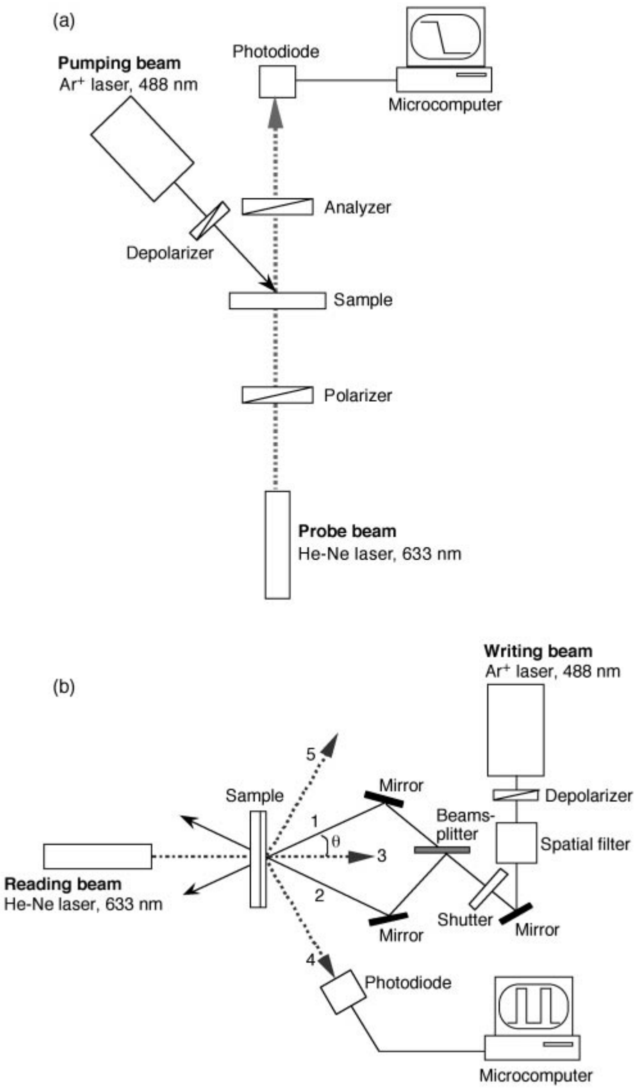

Fig. 2 (a) Experimental setup for the measurement of the photochemical phase transition behavior; (b) schematic illustration of the experimental setup for the formation of the real-time holographic grating.

Evaluation of formation of real-time holographic grating. Fig. 2(b) shows the holographic experimental setup. The grating was written by two unpolarized Ar$^+$ laser beams at 488 nm [beam 1 and 2 in Fig. 2(b)]. Turning on and off the two writing beams were controlled with a mechanical shutter with a response time of <0.5 ms. Two writing beams with an equal intensity were crossed in the sample film, and produced an interference pattern with a fringe spacing (Λ) which was estimated by eqn. (1),

$$\Lambda = \frac{\lambda}{2 \sin \theta} \tag{1}$$

where λ is the wavelength of the writing beam, and θ represents an incident angle of the writing beam. Under this condition, the resulting grating was the Raman–Nath (thin) grating regime, which is known to generate multiple orders of diffraction.[40] A linearly-polarized He–Ne laser (633 nm) with weak intensity was used as a reading beam [beam 3 in Fig. 2(b)], which was incident normal to the surface of the polymer film. Formation of the phase grating was monitored by measuring the power of the +1-order diffraction beam [beam 4 in Fig. 2(b)] with a photodiode, and the data were collected with a microcomputer. The diffraction efficiency, η, was determined by the ratio of the intensity of the diffraction beam to that of the reading beam.

Results and discussion

LC behavior of polymers

It was found that polymer 1 and polymer 2 exhibited liquid-crystalline behavior as evidenced by the DSC measurements, polarized microscopic observation and X-ray diffraction measurements. Polymer 1 showed optically anisotropic properties between 8 °C and 67 °C, and no diffraction peak was observed except for a broad halo around 20° in the X-ray diffraction pattern in this range of temperature. A similar tendency was also observed for polymer 2 between 118 °C and 131 °C. Both polymers exhibited a nematic phase. Phase structure and phase transition temperature of these PLCs are summarized in Table 1. In polymer 2, an optically anisotropic phase was also observed between 32 °C and 118 °C, at which only a broad halo around 20° was obtained in the X-ray diffraction patterns. Details of this phase are not clear at the present stage. It should be noted that the N–I phase transition temperature of polymer 1 with the siloxane spacer was lower than that of polymer 2 with only an alkyl spacer. It is suggested that introduction of the flexible side-chain spacer effectively decouples the motion of the polymer backbone from that of the anisotropically aligned mesogens, resulting in a decrease in the glass transition and the phase transition temperature of polymer 1.

Photochemical phase transition behavior of PLCs

Before investigation of formation of the grating with the PLCs, we confirmed their photochemical phase transition behavior. Fig. 3(a) shows the photochemical N–I phase transition and the thermal I–N phase transition behavior of polymer 1 at 60 °C. Before irradiation at 488 nm, a linearly polarized beam at 633 nm from a He–Ne laser could transmit through a pair of crossed polarizers, with the sample film between them, because of birefringence of polymer 1. The transmittance of the probe beam decayed immediately on irradiation at 488 nm in the N phase. This change in the transmittance indicates a decrease in the birefringence, resulting from the production of domains in which the N–I phase transition was induced by *trans–cis* photoisomerization of the azobenzene moiety. The transmittance of the probe beam recovered in about 10 min when photoirradiation was ceased. This is caused by the thermal I–N phase transition owing to the thermal *cis–trans* back-isomerization of the azobenzene moiety. A similar behavior was also observed for polymer 2 at 122 °C [Fig. 3(b)]. However, the degree of the N–I phase transition for polymer 1 was larger than that in polymer 2. The photochemical N–I phase transition is based on the orientational relaxation of mesogens caused by photochemical reaction of the azobenzene moieties. So the degree of the N–I phase transition is greatly affected by the amount of *cis*-azobenzenes produced upon photoirradiation. At present, there is a large difference in the irradiation temperature between polymer 1 and polymer 2, which will bring about the difference in the amount of *cis*-azobenzenes. The amount of *cis*-azobenzenes at high temperature is smaller than that at low temperature because of effective thermal *cis–trans* back-isomerization. Then the photochemical phase transition would not be effectively induced. The difference in the N–I phase transition behavior, therefore, would be due to the amount of *cis*-azobenzenes, resulting from the difference in the irradiation temperature.

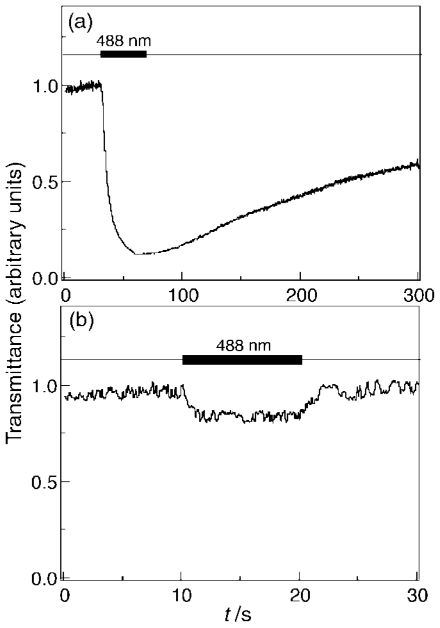

Fig. 3 Photochemical N–I phase transition and thermal I–N phase transition behavior of (a) polymer 1 and (b) polymer 2.

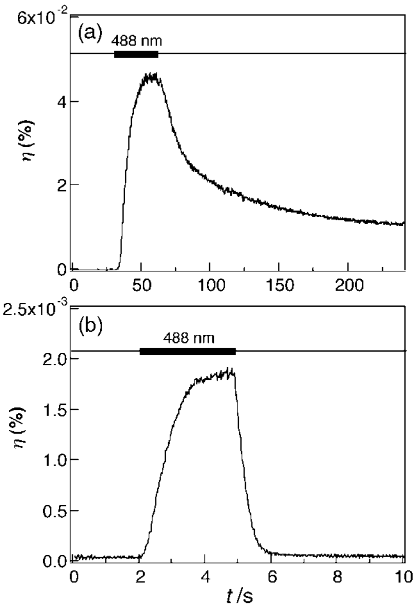

Fig. 4 Typical formation and removal of the holographic grating by turning on and off two writing beams: (a), polymer 1; (b), polymer 2.

Table 1 Thermodynamic properties and molecular weight of polymer liquid crystals[a]

	M_n	M_w/M_n	Phase transition temperature/°C	ΔH_{NI} (kJ mol^{-1})
Polymer 1	11 000	1.4	G 8 N 67 I	3.5
Polymer 2	13 700	1.3	G 32 X 118 N 131 I	1.7

[a] Abbreviations: M_n, number-average molecular weight; M_w, weight-average molecular weight; G, glass; X, unknown phase; N, nematic; I, isotropic; ΔH_{NI}, change in enthalpy of N–I phase transition.

Formation of real-time holographic grating

Formation of the holographic grating of polymer 1 and polymer 2 was investigated at 60 and 122 °C, respectively. Fig. 4(a) shows typical curves of the dynamic change in the +1-order diffraction efficiency for the thin film of polymer 1 as a function of time at the fringe spacing of 2.3 μm. Irradiation of the sample film with two writing beams (6.4 mW cm^{-2}) increased the diffraction efficiency, which indicates that the phase grating was created in the PLC film by interference of the two beams. The grating obtained could be removed gradually by turning off the writing beams. A similar result was also observed for polymer 2, as shown in Fig. 4(b). The grating in these PLCs could be obtained only in the sample film showing birefringence, eliminating the possibility of the thermal and population grating. Furthermore, it was found that the birefringence of the PLC film was decreased by production of the I domains which were photochemically induced as shown in Fig. 3. Therefore, such a formation of the grating would be due to induction of the photochemical N–I phase transition at bright regions of the interference pattern, leading to periodic change in the refractive index. On the other hand, removal of the grating would be achieved by recovery of the N phase due to *cis–trans* thermal back-isomerization.

It should be noted that the diffraction efficiency of polymer 1 was smaller than that of polymer 2. In general, the diffraction efficiency of index-of-refraction grating greatly depends on the degree of change in the refractive index (Δn), the thickness of the sample film (d) and the wavelength of the reading beam (λ), as shown by eqn. (2).[40]

$$\eta = \left(\frac{\pi d \Delta n}{\lambda}\right)^2 \tag{2}$$

In the present system, d of the PLC films was ~200 nm and λ was 633 nm; consequently, the smaller diffraction efficiency of polymer 1 may be closely related to Δn. The modulation of the refractive index is based on the photochemical N–I phase transition, so that Δn would depend on the degree of the N–I phase transition. As mentioned above, the formation of the grating with polymer 1 and polymer 2 was explored at 60 and 122 °C, respectively, resulting in the difference in the degree of the N–I phase transition between these PLCs. Therefore, the difference in the diffraction efficiency would be attributable to the difference in the photochemical phase transition behavior.

Next we evaluated the response time in the formation of the grating of these PLCs. The response time was defined as the time necessary to increase the intensity of the diffraction beam to 90% of the saturated value. It was found that the response time of polymer 1 and polymer 2 could be estimated as ~30 s and ~4 s, respectively. To qualitatively compare the rate of formation of the grating in both PLCs, the logarithmic plot of the rise response of the diffraction intensity was determined (Fig. 5). One can find that the rate of formation of the grating in polymer 1 is smaller than that in polymer 2, although the amount of the *cis*-azobenzene in polymer 1 would be larger than that in polymer 2. The photochemical phase transition is composed of two processes: the photochemical *trans–cis* isomerization of the azobenzene moiety and the orientational relaxation of the mesogens. In previous studies, we reported that the siloxane spacer scarcely affects the photoisomerization behavior,[30,31] so the difference in the rate of the PLCs may be related only to the orientational behavior of mesogens. As mentioned above, introduction of the siloxane spacer was effective to lower the temperature range of the LC phase of the polymers, in comparison with polymers having an alkyl spacer with the same backbone component and mesogens. This would be due to the low rotational energy barrier of the siloxane linkage. In the PLCs with the siloxane spacer, the mesogens would be aligned to stabilize the LC phase structure. Therefore, propagation of perturbation due to *trans–cis* photoisomerization of the azobenzene moiety in the LC phase would be suppressed, resulting in the small rate of the progress of the N–I phase transition.

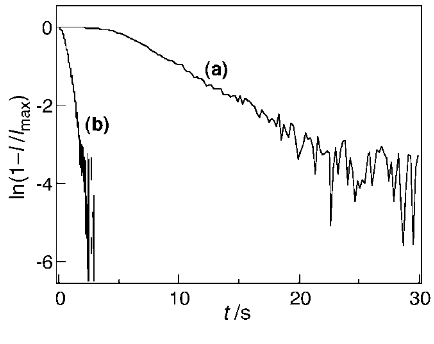

Fig. 5 Plot of logarithm of normalized diffraction signal *vs.* time for rise process: (a), polymer 1; (b), polymer 2.

Effect of incident angle of writing beams on grating

The effect of the incident angle of the writing beams on the diffraction efficiency was investigated (Fig. 6). The incident angle (θ) of each writing beam was varied from 15 to 6°, leading to the change in the fringe spacing from 0.94 to 2.8 μm. The efficiency was influenced by the fringe spacing and showed the maximum value at the spacing of 1.6 μm in polymer 1. The decrease in the diffraction efficiency at <1.6 μm may be attributable to the disappearance of Δn, which results from a decrease in the orientational order of the mesogens at dark regions by perturbation of the N–I phase transition. On the contrary, the origin of the decrease in the diffraction efficiency at >1.6 μm is not clear at this stage. On the other hand, a similar behavior was also obtained in polymer 2 without the siloxane spacer. The diffraction efficiency, however, showed a maximum value at the fringe spacing of 2.3 μm which was wider than the spacing obtained in polymer 1. Such a difference in the fringe spacing may be ascribed to the difference in structure of the spacer. As described above, the propagation of the perturbation of *cis*-azobenzenes in polymer 1 is suppressed due to the stabilized alignment of mesogens by the flexible siloxane spacer. Then the N–I phase transition induced at bright regions would little influence the alignment of mesogens at dark regions. On the other hand, the perturbation of *cis*-azobenzenes would be effectively propagated in polymer 2. So the N–I phase transition caused at the bright regions would affect the alignment of mesogens at the dark regions, resulting in the formation of a grating with a wider fringe spacing.

Effect of intensity of writing beams on grating

The effect of the intensity of the writing beam on the diffraction efficiency in polymer 1 and polymer 2 was evaluated at 60 and 122 °C, respectively. The beam intensity at 488 nm was varied

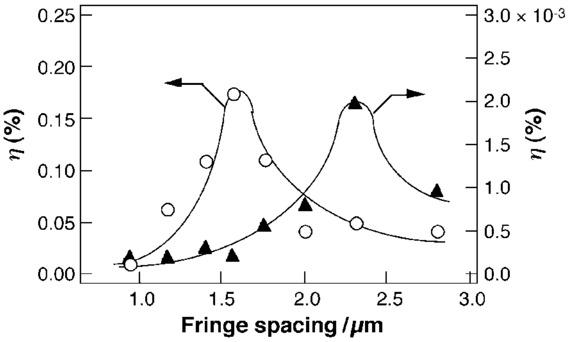

Fig. 6 Effect of fringe spacing on diffraction efficiency of polymer 1 (○) and polymer 2 (▲).

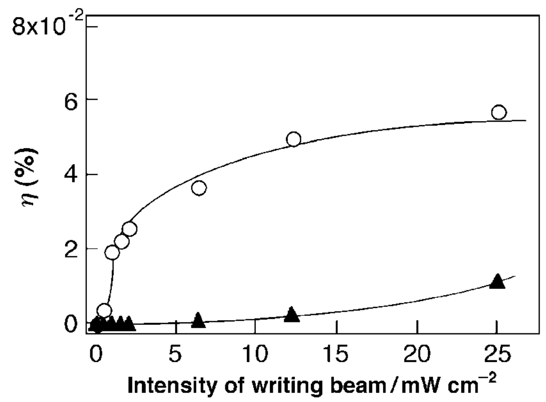

Fig. 7 Effect of intensity of writing beam on diffraction efficiency of polymer 1 (○) and polymer 2 (▲).

from 0.41 to 25 mW cm^{-2} by using neutral density filters. In both PLCs, the diffraction efficiency was clearly affected by the beam intensity, as shown in Fig. 7. In the present system, the diffraction efficiency depends only on Δn which is based on the N–I phase transition due to the *trans–cis* photoisomerization of the azobenzene moiety. The amount of *cis*-azobenzenes photochemically produced increases with increasing beam intensity, leading to enlargement of the degree of the N–I phase transition. Therefore, such dependence on the beam intensity would be ascribed to the difference in the degree of the photochemical N–I phase transition. It is worth noting that the beam intensity dependence greatly differed between these PLCs. In polymer 1, the grating could be created even at the intensity of 0.41 mW cm^{-2}, while the intensity of $>$6.4 mW cm^{-2} was required to produce the grating in polymer 2. This phenomenon can be explained in the same way as Fig. 4. Namely, the irradiation temperature of polymer 1 is lower than that of polymer 2 because the N–I phase transition temperature in polymer 1 is lowered from that in polymer 2 by introduction of the siloxane spacer. Such a lowering of the irradiation temperature brings about an increase in the amount of *cis*-azobenzenes produced upon photoirradiation, resulting in effective induction of the photochemical N–I phase transition. Consequently, this phenomenon is due to the difference in the N–I phase transition behavior based on the difference in the irradiation temperature.

Conclusion

In this article, the formation of a real-time holographic grating based on the photochemical phase transition was explored in the side-chain azobenzene PLC having a siloxane spacer. The introduction of the siloxane spacer lowered the N–I phase transition temperature of the PLC due to the flexibility of the siloxane units. This property resulted in a decrease in the irradiation temperature, leading to effective induction of the photochemical N–I phase transition following an increase in the amount of *cis*-azobenzenes. Therefore the formation of the grating in the PLC with the siloxane spacer could be achieved by a lower intensity of the writing beam than that in a conventional PLC including only an alkyl spacer. Furthermore, a grating with narrower fringe spacing could be created by suppression of the propagation of the perturbation owing to *trans–cis* isomerization of azobenzenes in the LC phase.

References

1 M. Eich and J. H. Wendorff, *Makromol. Chem. Rapid Commun.*, 1987, **8**, 59.
2 M. Eich and J. H. Wendorff, *Makromol. Chem. Rapid Commun.*, 1987, **8**, 467.
3 M. Eich and J. H. Wendorff, *J. Opt. Soc. Am. B*, 1990, **7**, 1428.
4 K. Anderle and J. H. Wendorff, *Mol. Cryst. Liq. Cryst.*, 1994, **243**, 51.
5 I. C. Khoo, S. Slussarenko, B. D. Guenther, M.-Y. Shih, P. Chen and W. V. Wood, *Opt. Lett.*, 1998, **23**, 253.
6 I. C. Khoo, *Opt. Lett.*, 1995, **20**, 2137.
7 I. C. Khoo, H. Li and Y. Liang, *Opt. Lett.*, 1994, **19**, 1723.
8 G. P. Wiederrecht, B. A. Yoon and M. R. Wasielewski, *Science*, 1995, **270**, 1794.
9 G. P. Wiederrecht, B. A. Yoon and M. R. Wasielewski, *Adv. Mater.*, 1996, **8**, 535.
10 G. P. Wiederrecht, B. A. Yoon, W. A. Svec and M. R. Wasielewski, *J. Am. Chem. Soc.*, 1997, **119**, 3358.
11 H. Ono and N. Kawatsuki, *Appl. Phys. Lett.*, 1997, **71**, 1162.
12 H. Ono, I. Saito and N. Kawatsuki, *Appl. Phys. Lett.*, 1998, **72**, 1942.
13 A. G. Chen and D. J. Brady, *Appl. Phys. Lett.*, 1993, **62**, 2920.
14 A. G. Chen and D. J. Brady, *Opt. Lett.*, 1992, **17**, 441.
15 X. Wei, X. Z. Yan, D. R. Zhu, D. Mo, Z. X. Liang and W. Z. Lin, *Appl. Phys. Lett.*, 1996, **68**, 1913.
16 A. Y.-G. Fuh, T.-C. Ko, M.-S. Tsai, C.-Y. Huang and L.-C. Chien, *J. Appl. Phys.*, 1998, **83**, 679.
17 S. Hvilsted, F. Andruzzi, C. Kulinna, H. W. Siesler and P. S. Ramanujan, *Macromolecules*, 1995, **28**, 2172.
18 L. Andruzzi, A. Altomare, F. Ciardelli, R. Solaro, S. Hvilsted and P. S. Ramanujan, *Macromolecules*, 1999, **32**, 448.
19 T. Bieringer, R. Wuttke and D. Haarer, *Macromol. Chem. Phys.*, 1995, **196**, 1375.
20 S. Kurihara, T. Ikeda, T. Sasaki, H.-B. Kim and S. Tazuke, *J. Chem. Soc., Chem. Commun.*, 1990, 1751.
21 T. Ikeda, T. Sasaki and H.-B. Kim, *J. Phys. Chem.*, 1991, **95**, 509.
22 S. Tazuke, S. Kurihara and T. Ikeda, *Chem. Lett.*, 1987, 911.
23 T. Ikeda, S. Horiuchi, D. B. Karanjit, S. Kurihara and S. Tazuke, *Macromolecules*, 1990, **23**, 42.
24 T. Ikeda and O. Tsutsumi, *Science*, 1995, **268**, 1873.
25 O. Tsutsumi, T. Shiono, T. Ikeda and G. Galli, *J. Phys. Chem. B*, 1997, **101**, 1332.
26 A. Shishido, O. Tsutsumi, A. Kanazawa, T. Shiono, T. Ikeda and N. Tamai, *J. Phys. Chem. B*, 1997, **101**, 2806.
27 A. Shishido, O. Tsutsumi, A. Kanazawa, T. Shiono, T. Ikeda and N. Tamai, *J. Am. Chem. Soc.*, 1997, **119**, 7791.
28 O. Tsutsumi, T. Kitsunai, A. Kanazawa, T. Shiono and T. Ikeda, *Macromolecules*, 1998, **31**, 355.
29 O. Tsutsumi, Y. Demachi, A. Kanazawa, T. Shiono, T. Ikeda and Y. Nagase, *J. Phys. Chem. B.*, 1998, **102**, 2869.
30 A. Kanazawa, A. Shishido, M. Hasegawa, O. Tsutsumi, T. Shiono, T. Ikeda, Y. Nagase, E. Akiyama and Y. Takamura, *Mol. Cryst. Liq. Cryst.*, 1997, **300**, 201.
31 A. Kanazawa, S. Hirano, A. Shishido, M. Hasegawa, O. Tsutsumi, T. Shiono, T. Ikeda, Y. Nagase, E. Akiyama and Y. Takamura, *Liq. Cryst.*, 1997, **23**, 293.
32 M. Engel, B. Hisgen, R. Keller, W. Kreuder, B. Reck, H. Ringsdorf, H. Schmidt and P. Tschirner, *Pure Appl. Chem.*, 1985, **57**, 1009.
33 C. Hsieh, C. Hsu, G. Hsiue and V. Percec, *J. Polym. Sci., Part A: Polym. Chem.*, 1990, **28**, 425.
34 Y. Nagase and Y. Takamura, *Makromol. Chem.*, 1992, **193**, 1225.
35 Y. Nagase, Y. Takamura, H. Abe, K. Ono, T. Saito and E. Akiyama, *Makromol. Chem.*, 1993, **194**, 2517.
36 E. Akiyama, M. Yamazaki, Y. Takamura and Y. Nagase, *Makromol. Chem. Rapid Commun.*, 1994, **15**, 161.
37 E. Akiyama, Y. Takamura and Y. Nagase, *Polym. J.*, 1994, **26**, 1277.
38 V. P. Shibaev, S. G. Kostromin and N. A. Plate, *Eur. Polym. J.*, 1982, **18**, 651.
39 H. Ringsdorf and H. W. Schmidt, *Makromol. Chem.*, 1984, **185**, 1327.
40 H. J. Eichler, P. Günther and D. W. Pohl, in *Laser Induced Dynamic Grating*, Springer-Verlag, Berlin, 1986.

Paper 9/03948A